Plant Glutathione Peroxidases Are Functional Peroxiredoxins Distributed in Several Subcellular Compartments and Regulated during Biotic and Abiotic Stresses[1][W]

Nicolas Navrot, Valérie Collin, José Gualberto, Eric Gelhaye, Masakazu Hirasawa, Pascal Rey, David B. Knaff, Emmanuelle Issakidis, Jean-Pierre Jacquot, and Nicolas Rouhier*

Unité Mixte de Recherche Institut National de la Recherche Agronomique-Université Henri Poincaré 1136, Interactions Arbres/Micro-organismes, Institut de Formation et de Recherche 110 Génomique, Ecophysiologie et Ecologie Fonctionnelles, Université Henri Poincaré, Faculté des Sciences, 54506 Vandoeuvre cedex, France (N.N., E.G., J.-P.J., N.R.); Commissariat à l'Energie Atomique/Cadarache, Direction des Sciences du Vivant, Département d'Ecophysiologie Végétale et de Microbiologie, Laboratoire d'Ecophysiologie Moléculaire des Plantes, 13108 Saint-Paul-lez-Durance cedex, France (V.C., P.R.); Institut de Biologie Moléculaire des Plantes, Centre National de la Recherche Scientifique, 67084 Strasbourg cedex, France (J.G.); Department of Chemistry and Biochemistry, and Center for Biotechnology and Genomics, Texas Tech University, Lubbock, Texas 79409–1061 (M.H., D.B.K.); and Institut de Biotechnologie des Plantes, Unité Mixte de Recherche 8618, Université de Paris Sud, 91405 Orsay cedex, France (E.I.)

We provide here an exhaustive overview of the glutathione (GSH) peroxidase (Gpx) family of poplar (*Populus trichocarpa*). Although these proteins were initially defined as GSH dependent, in fact they use only reduced thioredoxin (Trx) for their regeneration and do not react with GSH or glutaredoxin, constituting a fifth class of peroxiredoxins. The two chloroplastic Gpxs display a marked selectivity toward their electron donors, being exclusively specific for Trxs of the y type for their reduction. In contrast, poplar Gpxs are much less specific with regard to their electron-accepting substrates, reducing hydrogen peroxide and more complex hydroperoxides equally well. Site-directed mutagenesis indicates that the catalytic mechanism and the Trx-mediated recycling process involve only two (cysteine [Cys]-107 and Cys-155) of the three conserved Cys, which form a disulfide bridge with an oxidation-redox midpoint potential of −295 mV. The reduction/formation of this disulfide is detected both by a shift on sodium dodecyl sulfate-polyacrylamide gel electrophoresis or by measuring the intrinsic tryptophan fluorescence of the protein. The six genes identified coding for Gpxs are expressed in various poplar organs, and two of them are localized in the chloroplast, with one colocalizing in mitochondria, suggesting a broad distribution of Gpxs in plant cells. The abundance of some Gpxs is modified in plants subjected to environmental constraints, generally increasing during fungal infection, water deficit, and metal stress, and decreasing during photooxidative stress, showing that Gpx proteins are involved in the response to both biotic and abiotic stress conditions.

In plant cells, aerobic reactions such as photosynthesis or respiration lead to reactive oxygen species (ROS) production. These ROS, such as superoxide radicals, hydroxyl radicals, or hydrogen peroxide (H_2O_2), can damage biological molecules, including nucleic acids, lipids, and proteins. Rates of ROS generation and cellular ROS levels both increase greatly when plants are subjected to environmental or biotic stresses. Plants have developed several nonenzymatic and enzymatic systems to protect against oxidative damage caused by these ROS. Carotenoids, tocopherols, glutathione (GSH), and ascorbate are the major nonenzymatic antioxidant compounds (Noctor and Foyer, 1998). Enzymatic systems include superoxide dismutases, catalases, ascorbate peroxidases, and peroxiredoxins (Prxs), also named thioredoxin (Trx) peroxidases.

Usually, plant Prxs are classified as belonging to one of four subgroups, called 2-Cys Prx, 1-Cys Prx, type II Prx, and Prx Q. They were initially identified by sequence analysis (i.e. on the number and position of conserved Cys) and on the catalytic mechanism used for peroxide reduction (Rouhier and Jacquot, 2002). All Prxs display a conserved catalytic Cys, located in the N-terminal portion of the protein, which is first

[1] This work supported by the Robert A. Welch Foundation (work carried out at Texas Tech University; grant no. D–0710 to D.B.K.), by Commissariat à l'Energie Atomique (program Toxicologie Nucléaire Environnementale), by MENRT (grant to N.N.), and by BQR Région Lorraine (to N.R., J.P.J., and E.G.).

* Corresponding author; e-mail nrouhier@scbiol.uhp-nancy.fr.

The author responsible for distribution of materials integral to the findings presented in this article in accordance with the policy described in the Instructions for Authors (www.plantphysiol.org) is: Nicolas Rouhier (nrouhier@scbiol.uhp-nancy.fr).

[W] The online version of this article contains Web-only data.

www.plantphysiol.org/cgi/doi/10.1104/pp.106.089458

transformed into a sulfenic acid after peroxide reduction. The main difference between the various groups of plant Prxs is the mechanism of regeneration of the reduced enzyme. For the 2-Cys Prx class, the sulfenic acid is reduced via the formation of an intermolecular disulfide bridge using a resolving Cys found on another subunit, whereas for the Prx Q class, the resolving Cys is located on the same subunit and forms an intramolecular disulfide bridge (Rouhier and Jacquot, 2002). In most cases, these disulfides are then reduced via the Trx system. For the two other classes, the sulfenic acid is likely to be reduced without formation of a disulfide bond, as there is no other strictly conserved Cys involved in catalysis. One major difference between these two classes of plant Prxs is that type II Prxs are reduced by the glutaredoxin (Grx) or the Trx system or both (Rouhier et al., 2001; Brehelin et al., 2003; Finkemeier et al., 2005), whereas the 1-Cys Prxs seem to be reduced only by the Trx system (Pedrajas et al., 2000).

Recent studies have shown that some plant and yeast (*Saccharomyces cerevisiae*) GSH peroxidases (Gpx) can reduce peroxides, much more efficiently or sometimes exclusively, by using the Trx system rather than GSH as a reductant (Herbette et al., 2002; Jung et al., 2002; Tanaka et al., 2005). In the unicellular parasite *Plasmodium falciparum*, a Gpx-like protein, closely related to plant Gpxs, has also been shown to be specific for Trx as a reductant (Sztajer et al., 2001). Thus, in a classification based on biochemical feature rather than on phylogenetic linkage, the plant Gpxs constitute a fifth group of Prxs (Rouhier and Jacquot, 2005).

Most of the Gpxs found in animal cells are well-characterized selenium-containing enzymes. Because of the high reactivity of the active site seleno-Cys, enzymes of this family are among the most efficient antioxidant systems in animal cells (Maiorino et al., 1990). One of these selenium-containing enzymes has also been found in a unicellular photosynthetic organism, the green alga *Chlamydomonas reinhardtii* (Fu et al., 2002; Novoselov et al., 2002). In higher plants, the Gpx-like proteins identified so far possess a Cys instead of a seleno-Cys at their active site. Some studies showing that plant Gpxs are far less reactive than their animal counterparts have attributed the lower activity of plant Gpxs to the lower reactivity of Cys compared to seleno-Cys (Eshdat et al., 1997). However, replacement of the active-site Cys with seleno-Cys did not significantly increase the GSH-dependent peroxidase activity of a citrus Gpx (Hazebrouck et al., 2000). Thus, at least in some cases, other differences between animal and plant enzymes exist and produce different biochemical properties. Avery et al. (2004) have shown some gaps in the amino acid sequences of yeast Gpxs compared to mammalian Gpxs, raising the possibility of some important biochemical differences between these two types of Gpxs. It should also be noted that yeast and plant Gpxs may play a role distinct from that of their animal counterparts and could be part of an alternative pathway that scavenges peroxides, especially phospholipid hydroperoxides (Eshdat et al., 1997).

The level of Gpx mRNA from various organisms is affected by stress conditions (Criqui et al., 1992; Holland et al., 1994; Sugimoto and Sakamoto, 1997; Depege et al., 1998; Roeckel-Drevet et al., 1998; Li et al., 2000; Agrawal et al., 2002; Rodriguez Milla et al., 2003; Kang et al., 2004). Other studies have followed changes in Gpx activity in stress conditions (Aravind and Prasad, 2005; Kuzniak and Sklodowska, 2005; Ali et al., 2006; Gajewska and Sklodowska, 2006). In these studies, the Gpx expression or activity is generally up-regulated in response to stress. However, there are exceptions to this pattern. For example, while the expression of two Gpx isoforms increases in barley (*Hordeum vulgare*) under osmotic or methyl viologen-induced stress, a third Gpx isoform (HVGPH3) is down-regulated under these conditions (Churin et al., 1999). These proteins may thus have different functions in plant cells, with one or more isoforms functioning in a signal transduction pathway, while other isoforms serve as enzymes involved in catalyzing modification of potentially harmful stress-related chemical agents. A signal-transducing role for a Gpx has already been demonstrated in yeast, which possesses three plant-type Gpxs, where Gpx3 functions as a redox sensor and is involved in gene activation by regulating the AP1 transcription factor (Delaunay et al., 2002).

The annotation of the first release of the poplar (*Populus trichocarpa*) genome indicates the presence of six complete *Gpx* genes. To understand why so many Trx-dependent peroxidases are present in plant cell compartments, we first focused our attention on the specificity of Gpx proteins toward different electron donors and substrates. All of them use Trx but not GSH as a donor, but most importantly, a specific interaction was found between chloroplastic Gpxs and y-type Trxs. No specificity was observed with regard to substrates. Moreover, we have demonstrated that only two of the three conserved Cys present in plant Gpxs participate in the catalytic cycle and in Trx-mediated regeneration. The subcellular localization of two Gpx isoforms was characterized by green fluorescent protein (GFP) fusions in two distinct subcellular compartments, and the gene expression and protein abundance were analyzed in various plant tissues and stress conditions. The amount of some Gpxs is modified upon pathogen infection and in response to water deficit and photooxidative and metal stresses, revealing their participation in stress responses.

RESULTS

Sequence and Genome Analysis

Five different isoforms of Gpx, termed PtrcGpx 1 to 5 (for poplar Gpx) were initially identified in the different poplar expressed sequence tag (EST) databases available. With the recent release of the first version of the poplar genome sequence by the Department of

Energy (DOE) Joint Genome Institute (JGI), a sixth isoform, very similar to PtrcGpx3, was identified, and these two isoforms were named PtrcGpx3.1 and PtrcGpx3.2. The only obvious difference between the two sequences is the presence of an N-terminal extension in PtrcGpx3.2, otherwise they are 90% identical and display a 99% functional homology in their predicted mature form. The protein sequences of all poplar Gpxs identified are shown in Figure 1 and compared with Gpxs from yeast and human. The percentage of strict identity ranges from 62% to 90% among all poplar Gpxs and from 20% to 48% versus yeast and mammalian Gpxs. The lengths of the proteins vary from 168 to 238 amino acids, depending on the presence of N-terminal extensions in some isoforms.

From this amino acid sequence comparison, it appears that poplar Gpxs are more closely related to yeast Gpxs than to human Gpxs. Indeed, three Cys (residues generally assumed to be essential for Gpx catalysis) are not only strictly conserved in all poplar Gpxs but also in all higher plant and yeast sequences (Fig. 1; data not shown). This is in clear contrast to animal Gpxs, which display either two conserved Cys residues or in some isoforms a Cys and a seleno-Cys. The difference in the number of conserved Cys could result in different reactivities for plant and yeast Gpxs compared to mammalian enzymes. The closest human homolog to plant and yeast Gpxs is Gpx4, also known as phospholipid hydroperoxide Gpx. Some residues are highly conserved in all these sequences, especially in the neighborhood of the two first conserved Cys (the respective consensus sequences are VASx[C/U]G and FPCNQF, with U being the symbol for seleno-Cys). The three residues, Gly, Gln, and Trp denoted with asterisks in Figure 1, which are involved in the catalytic mechanism of the mammalian seleno-Gpxs (Prabhakar et al., 2005), are also conserved in plant and yeast sequences. However, no information is available about the role of these residues in plant or yeast Gpxs.

Another interesting feature, arising from the poplar genome release, is that the *gpx* gene structure is very conserved in poplar. All the genes contain six exons of almost the same length, whereas the size of the intron sequences varies greatly. The major differences are found in the first exon, because it includes putative targeting sequences for some isoforms (Supplemental Table S1). Another difference is the slightly smaller size of exon 6 for *PtrcGpx1* (30 nucleotides instead of 33 in the other *Gpx* sequences, resulting in a PtrcGpx1 sequence shortened by one amino acid in the C terminus). This organization is similar in Arabidopsis (*Arabidopsis thaliana*), where the eight genes also contain six exons. In Arabidopsis, the last exon is also shorter for some genes, in particular for the homologs of *PtrcGpx1* (Rodriguez Milla et al., 2003; data not shown).

Some characteristics of poplar Gpxs are summarized in Table I. The consensus subcellular predictions obtained with different software (Predotar, TargetP, Mitoprot, and Psort) are as follows: PtrcGpx1 carries a putative plastidic transit peptide; PtrcGpx3.2, a mitochondrial or plastidic one; and PtrcGpx2 and PtrcGpx5, a peptide presumably directing the proteins into the secretory pathways, whereas PtrcGpx4 and PtrcGpx3.1 should be localized in the cytosol.

We then built a phylogenetic tree using most of the plant Gpx sequences present in the databases with an emphasis on the eight and five Gpxs identified in Arabidopsis and *Oryza sativa* genomes, respectively (Fig. 2). Although the tree was constructed using sequences devoid of N-terminal extensions, five subgroups of Gpx, which are likely to correspond to the predicted intracellular protein localization, can be defined. This means that there are probably some amino acid signatures specific for each subgroup. It also appears that some organisms possess two members of the same group. For example, Arabidopsis has two putative chloroplastic and two cytosolic Gpxs, explaining the higher gene content in this plant. In contrast, the subgroup including the predicted secreted proteins is not found in *O. sativa*.

Biochemical Characterization

We have cloned five of the six Gpx sequences, minus their N-terminal extensions, in the pET-3 d plasmid for subsequent expression in *Escherichia coli*. Because of the high similarity between PtrcGpx3.1 and PtrcGpx3.2, we have only expressed the mature form of PtrcGpx3.2, which was the most abundant in terms of ESTs and also the first identified. The sizes of the mature forms that we have expressed range from 164 to 171 amino acids. All the proteins, except PtrcGpx2, were soluble. After purification to homogeneity, the yields ranged from 5 mg for PtrcGpx2 (after resolubilization from inclusion bodies) to about 100 mg of protein/L culture for the other isoforms.

Electron Donor Specificity

As it was demonstrated earlier that Trx was a better electron donor than GSH for some Gpx-like proteins, we have tested different electron donor systems, i.e. the Trx and Grx systems or GSH alone. We have first measured the Gpx activity using a spectrophotometric test coupled to NADPH oxidation.

Except for PtrcGpx2, which was completely inactive, all the proteins (PtrcGpx1, PtrcGpx3.2, PtrcGpx4, and PtrcGpx5) catalyzed H_2O_2 reduction at similar rates using poplar Trx h1 as the electron donor, NADPH, and recombinant Arabidopsis type B NADPH-thioredoxin reductase (data not shown; Table II). In contrast, no activity was found when using either GSH alone or in combination with different poplar Grxs belonging to the same subgroup, either dithiol Grx with a classical CxxC active site (Grx C1, C2, C3, and C4) or a monothiol chloroplastic Grx (Grx S12), which possesses a CxxS active site (see Rouhier et al., 2006 for the nomenclature; data not shown).

Because all recombinant proteins, with the exception of PtrcGpx2, were equally active in transferring

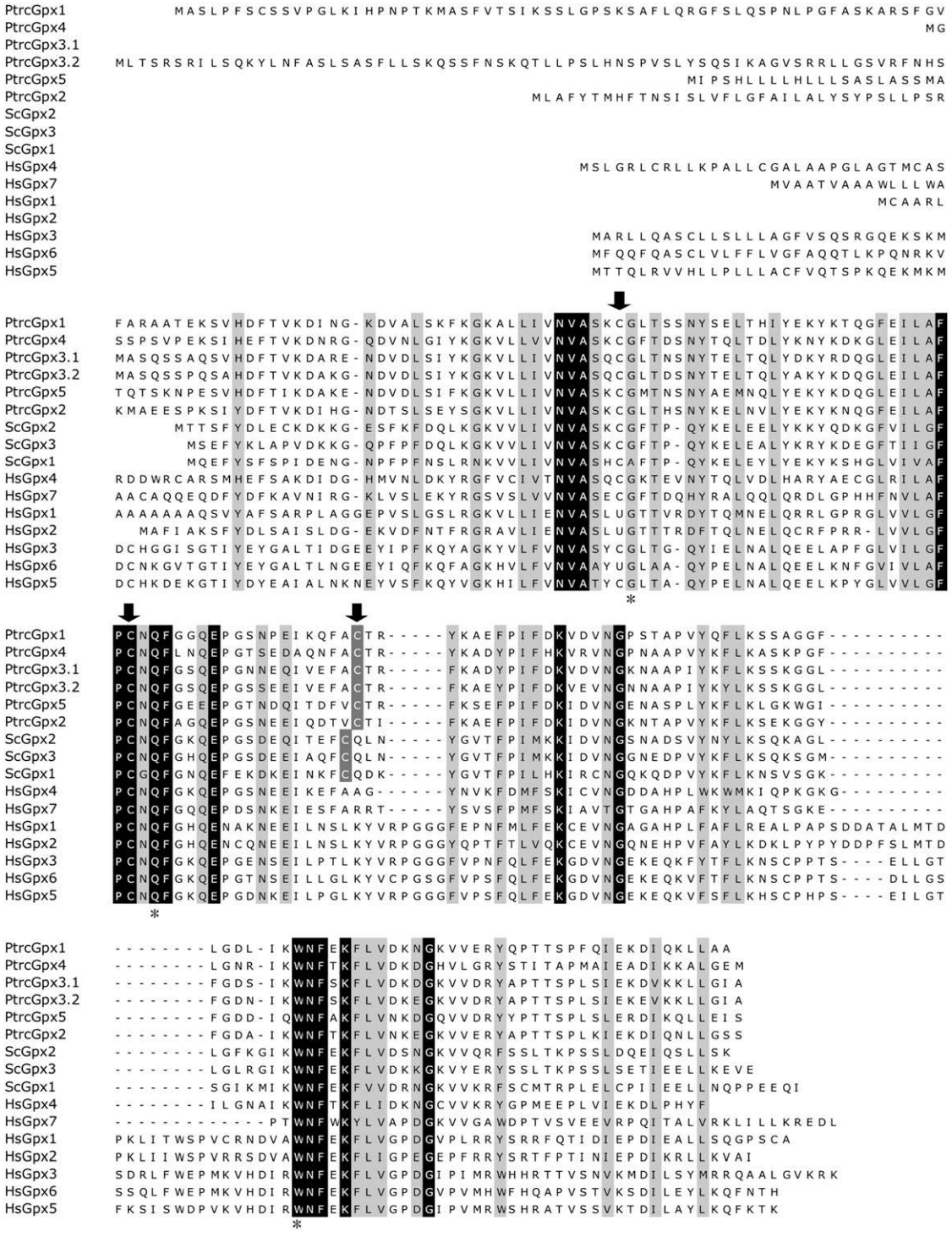

Figure 1. Amino acid sequence alignment of Gpxs from poplar, yeast, and human. Poplar Gpx gene models from DOE JGI *Populus trichocarpa* v1.0 database (http://genome.jgi-psf.org/Poptr1/Poptr1.home.html): PtrcGpx1, grail3.0013048601; PtrcGpx2, estExt_Genewise1_v1.C_LG_VII0868; PtrcGpx3.1, estExt_Genewise1_v1.C_LG_I8960; PtrcGpx3.2, fgenesh4_kg.C_LG_III000037; PtrcGpx4, estExt_fgenesh4_kg.C_LG_XIV0026; PtrcGpx5, eugene3.00010913. Accession numbers of yeast and human Gpx: ScGpx1, P36014; ScGpx2, P38143; ScGpx3, NP012303; HsGpx1, P07203; HsGpx2, AAH05277; HsGpx3, P22352; HsGpx4, NP_002076; HsGpx5, NP_001500; HsGpx6, NP_874360. Strictly conserved amino acids are on black background, functionally conserved amino acids are on gray background. Arrows show the three conserved Cys in positions 107, 136, and 155 (PtrcGpx1 numbering). Asterisks show three residues involved in the catalytic mechanism in human selenoenzyme. U indicates seleno-Cys in human enzymes.

Table I. *Characteristics of poplar Gpxs*

The molecular masses of the recombinant mature proteins are indicated. The masses of the full-length proteins including signal peptide are in parentheses. Poplar gene models were found in the DOE JGI poplar v1.0 database. Arabidopsis homologs are named according to Rodriguez Milla et al. (2004), except for AtGpx8, which was not described in this paper. *O. sativa* homologs were found using the Institute for Genomic Research *O. sativa* genome annotation database (http://www.tigr.org/tdb/e2k1/osa1/index.shtml). The localization predictions are the consensus from results obtained with Predotar (http://genoplante-info.infobiogen.fr/predotar/predotar.html), TargetP (http://www.cbs.dtu.dk/services/TargetP/), Mitoprot (http://ihg.gsf.de/ihg/mitoprot.html), and WoLF Psort (http://wolfpsort.seq.cbrc.jp/) software. Ptrc, Poplar.

Protein	Gene Model	Length (Amino Acids)	Molecular Mass	EST No.	Predicted Localization	Predicted TP Length	Arabidopsis Homolog	*O. sativa* Homolog
			D					
PtrcGpx1	grail3.0013048601	164 (232)	18,250 (25,359)	48	Chloroplastic	71	AtGPX1 (At2g25080), AtGPX7 (At4g31870)	LOC_Os06g08670
PtrcGpx2	estExt_Genewise1_v1.C_LG_VII0868	170 (203)	18,842 (22,850)	10	Secreted	38	AtGPX2 (At2g31570), AtGPX3 (At2g43350)	LOC_Os11g18170
PtrcGpx3.1	estExt_Genewise1_v1.C_LG_I8960	168	18,691	23	Cytosolic	–	AtGPX6 (At4g11600)	LOC_Os04g46960 LOC_Os02g44500
PtrcGpx3.2	fgenesh4_kg.C_LG_III000037	168 (238)	18,550 (26,306)	85	Mitochondrial chloroplastic	70	AtGPX6 (At4g11600)	LOC_Os04g46960 LOC_Os02g44500
PtrcGpx4	estExt_fgenesh4_kg.C_LG_XIV0026	171	18,950	17	Cytosolic	–	AtGPX4 (At2g48150), AtGPX5 (At3g63080)	LOC_Os03g24380
PtrcGpx5	eugene3.00010913	169 (203)	19,250 (21,498)	8	Secreted	31	AtGPX8 (At1g63460)	–

electrons from reduced Trx to H_2O_2, only one of them, PtrcGpx3.2, was selected for more detailed study.

As PtrcGpx3.1, the cytosolic isoform, is very similar in sequence to PtrcGpx3.2, we tested in vitro various cytosolic Trxs of the h type in an attempt to find a potential physiological electron donor for this protein, using NADPH oxidation coupled to the NTR-catalyzed reduction of Trx to monitor activity. All the poplar Trx h tested (Trx h1, h3, and h5) are efficient electron donors for PtrcGpx3.2 in vitro, with apparent K_m values being around 10 μM (Table II). It was previously shown that Trx h2, although it colocalizes with PtrcGpx3.2 in mitochondria, is a very poor electron donor (Gelhaye et al., 2004). We next tried to identify a preferred, and hopefully physiological, electron donor for the two chloroplastic Gpxs, PtrcGpx1 and PtrcGpx3.2. A colorimetric method was used for these assays as an alternative to the assay based on monitoring NADPH oxidation, because chloroplastic Trxs are reduced by a light-dependent system involving ferredoxin and ferredoxin Trx reductase. As chloroplastic Trxs are not reduced by NTR, the reducing capacity of Arabidopsis chloroplastic Trxs was tested in the presence of 500 μM dithiothreitol (DTT), a reagent that will reduce these Trxs but does not support the peroxidase activity of Gpxs during the relatively short time used for the assay. Of all the chloroplastic Trxs tested, only the two Arabidopsis y-type Trxs (Trx y1 and Trx y2) were able to reduce Gpx to a significant extent. Similar results were obtained for PtrcGpx1 and PtrcGpx3.2, with the reduced y-type Trxs leading to an 80% decrease of the H_2O_2 content with both Gpxs (Fig. 3; data not shown). The other isoforms tested did not support Gpx activity. The cytosolic poplar Trx h1, present at the same concentration as the chloroplastic Trxs, was approximately as effective as the y-type Trxs in supporting H_2O_2 reduction catalyzed by either PtrcGpx1 or PtrcGpx3.2. Despite the similar reactivity of the cytoplasmic Trx h1, the fact that the two y-type Trxs present in the poplar genome colocalize with PtrcGpx1 and PtrcGpx3.2 in chloroplasts suggests that the two Trx y may well constitute in vivo reductants for these two Gpxs.

Peroxide Specificity

The substrate specificity of PtrcGpx3.2 was tested under steady-state conditions using Trx h1 as reductant and different types of peroxides, ranging from H_2O_2 to more complex molecules, such as tert-butyl hydroperoxide (tBOOH) or cumene hydroperoxide (COOH), as electron acceptors. The K_m values for the different substrates and the catalytic efficiencies of the enzymes are summarized in Table II. Although slightly different (K_m ranging from 239 μM to 1.41 mM), the K_m values for the three substrates are all of the same order of magnitude in the millimolar range. In terms of catalytic efficiency (k_{cat}/K_m), PtrcGpx3.2 is slightly more efficient in reducing COOH (5.3×10^4 M^{-1} s^{-1}) compared to H_2O_2 (20×10^3 M^{-1} s^{-1}) and to tBOOH (6.4×10^3 M^{-1} s^{-1}).

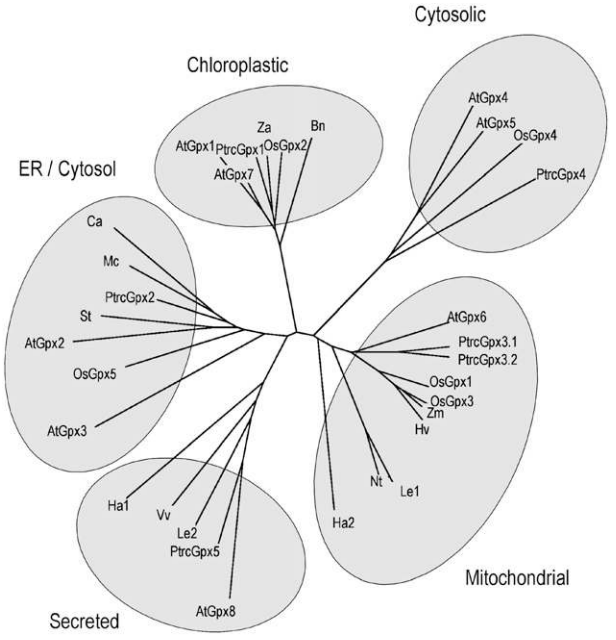

Figure 2. Phylogenetic tree of plant Gpxs. The gene models used for poplar Gpxs are indicated in Figure 1. The other accession numbers (full-length cDNAs or ESTs) are as follows. Arabidopsis: AtGpx1, At2g25080; AtGpx2, At2g31570; AtGpx3, At2g43350; AtGpx4, At2g48150; AtGpx5, At3g63080; AtGpx6, At4g11600; AtGpx7, At4g31870; AtGpx8, At1g63460. *O. sativa*: OsGpx1, AY100689; OsGpx2, CB666847; OsGpx3, CF306402; OsGpx4, CF281628; OsGpx5, AAX96834. *Helianthus annuus*: Ha1, CAA74775; Ha2, CAA75009. *L. esculentum*: Le1, BI209257; Le2, AI898013. *Brassica napus*: AF411209. Ca, *Cicer arietinum*, CAD31839; Hv, *H. vulgare*, BJ448530; Mc, *Momordica charantia*, AF346906; Nt, *N. tabacum*, CK286614; St, *Solanum tuberosum*, BM404021; Vv, *Vitis vinifera*, CB978870; Za, *Zantedeschia aethiopica*, AAC78466; Zm, *Zea mays*, BI319059. Only the predicted mature sequences were used for tree building.

We then examined the stoichiometry of the reaction catalyzed by Gpxs, by mixing known concentrations of reduced enzyme with various known concentrations of tBOOH in the absence of reductants. After completion of the reaction, the remaining peroxide content was measured using the ferrous oxidation of xylenol orange (FOX) colorimetric method. All the enzymes tested (PtrcGpx1, 3.2, and 5) can reduce 1 mol substrate per mole enzyme, indicating that Gpxs use only one or two Cys but certainly not three.

It is known that, for enzymes that use sulfenic acid chemistry for their catalysis, the stoichiometry depends on the number of Cys involved. When one or two Cys are involved, the stoichiometry of the reaction is 1 mol of enzyme oxidized per mol of peroxide reduced (Boschi Muller et al., 2000). In one case, the first peroxidatic Cys attacks the substrate and is converted to a sulfenic acid, with the reaction stopping at this point. More commonly, a second resolving Cys attacks the sulfenic acid, leading to the formation of a disulfide bridge. When a third Cys is involved in the catalytic mechanism, as it is the case for some Met sulfoxide reductases, the stoichiometry of the reaction is 2 (Boschi Muller et al., 2005). In this case, the third Cys (or the second resolving Cys) reduces the first disulfide bridge formed between the peroxidatic Cys and the first resolving Cys, leading to a new intramolecular bridge. Then, the peroxidatic Cys would be free and able to attack another molecule of peroxide, leading to a consumption of 2 mol peroxide per mole of reduced enzyme.

Catalytic Mechanism

To understand the mechanism used by PtrcGpxs for peroxide reduction and for the Trx-dependent regeneration, site-directed mutagenesis was used to generate four variants of PtrcGpx3.2 (PtrcGpx3.2 C107S, C136S, C155, or C136/155S) in which Cys residues were replaced by Sers. The activity of the mutated proteins was tested in the presence of the Trx system. As expected, the Cys 107S mutant is totally inactive. While PtrcGpx3.2 C155S or the double mutant PtrcGpx3.2 C136/155S are able to reduce peroxides in single-turnover experiments (i.e. prereduced samples of these two variants can reduce an equal amount of peroxide), they are completely inactive with the Trx-reducing system, regardless of the peroxide substrate used. This indicates that Trx is probably not able to directly reduce the sulfenic acid formed on Cys-107. In contrast, PtrcGpx3.2 C136S displays almost identical enzymatic properties to PtrcGpx3.2 (Table II). The only difference is a small modification of the K_m value for peroxides that results in a decreased catalytic efficiency. These results indicate unequivocally that Cys-107 and Cys-155 are required for Trx regeneration, whereas Cys-136, albeit strictly conserved and found in a very conserved motif, does not have a catalytic role.

Table II. *Steady-state kinetic parameters of PtrcGpx3.2 and PtrcGpx3.2 C136S*

Values for the different peroxides were obtained using Trx h1 as electron donor. A total of 200 nM of enzyme was used in the tests. PtrcGpx C107S, C155S, and C136/155S mutants are inactive with the Trx system.

		K_m	k_{cat}	k_{cat}/K_m
		mM	s^{-1}	$(M^{-1}\ s^{-1}) \times 10^3$
H_2O_2	PtrcGpx3.2	0.545	11	20
	PtrcGpx3.2 C136S	1.388	13	12
tBOOH	PtrcGpx3.2	1.41	9.08	6.4
	PtrcGpx3.2 C136S	4.66	12	2.6
COOH	PtrcGpx3.2	0.239	13	53
	PtrcGpx3.2 C136S	0.454	16	35
		K_m		
		μM		
tBOOH	Trx h1	12		
	Trx h3	13		
	Trx h5	10.3		

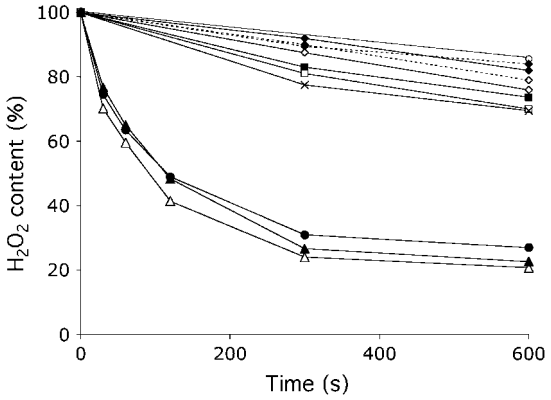

Figure 3. Time-course-dependent H_2O_2 reduction by PtrcGpx1 in the presence of chloroplastic Trxs. Activity of PtrcGpx1 was tested using different chloroplastic Arabidopsis Trxs by following H_2O_2 consumption in function of time. Reactions contain 2 μM PtrcGpx1, 500 μM DTT, 400 μM H_2O_2, and 10 μM of the different Arabidopsis Trx. From top to bottom: control without addition of Trx (○), Trx m3 (◆, dotted line), Trx m1 (◆), Trx m4 (◇, dotted line), Trx m2 (◇),Trx f1 (■), Trx f2 (□), Trx x (x), poplar Trx h1(●), Trx y2 (▲), and Trx y1 (△).

Redox and Oligomerization States

We examined the behavior of PtrcGpx3.2 and its various Cys/Ser variants during denaturing polyacrylamide gel electrophoresis (SDS-PAGE) under different conditions. Under reducing conditions (30 mM DTT), all the proteins migrated at their expected molecular masses, around 19 kD (Fig. 4A, lanes 2, 4, 6, 8, and 10). Under oxidizing conditions (30 mM H_2O_2), the migration of PtrcGpx3.2, as well as of its C107S and C136S variants, is shifted to a lower apparent molecular mass (around 13 kD), whereas the migration of C155S and C136S/155S mutated proteins was not altered (Fig. 4A, lanes 1, 3, 5, 7, and 9). The change in the migration profile under oxidizing conditions for all the proteins in which Cys-155 has not been mutated suggests that an intramolecular disulfide bond involving Cys-155 can be formed. The disulfide, formed between Cys-107 and Cys-155 in the case of the C136S mutant and between Cys-136 and Cys-155 in the case of the C107S mutant, apparently modifies the overall structure of the proteins sufficiently to alter the migration behavior during electrophoresis. It should also be pointed out that a covalent dimer, involving Cys-107 of two subunits, can be observed for the double mutant under nonreducing conditions but not under reducing conditions, as has been previously observed for mutated proteins in which only the catalytic Cys remains (Rouhier et al., 2004). These results were confirmed by following changes in intrinsic Trp fluorescence emission of the proteins in reduced or oxidized conditions (Fig. 4B). Only one Trp found in position 196 in the WNF motif and conserved among organisms is present in PtrcGpx3.2. The behavior of PtrcGpx3.2 is shown in Figure 4B as an example, but all Gpxs behave similarly. While the protein is in the oxidized form after purification (the number of detectable thiol groups is generally close to zero), adding 250 μM DTT changed the emission fluorescence spectrum of the protein, with a decrease of approximately 3-fold in the fluorescence intensity and a shift of the maximum of fluorescence emission from 350 to 316 nm. The addition of 250 μM peroxide in the cuvette completely restored the initial spectrum, suggesting that changes of Trp environment and thus of fluorescence emission are linked to changes in oxidation state. Among the cysteinic-mutated proteins, only PtrcGpx3.2 C136S showed similar differences in the fluorescence properties of the oxidized and reduced forms. All other mutated proteins (PtrcGpx3.2 C107S, PtrcGpx3.2 C155S, and PtrcGpx3.2 C136S/155S) did not share this property (data not shown). As observed under SDS-PAGE, where it abolished the shift between oxidized and reduced

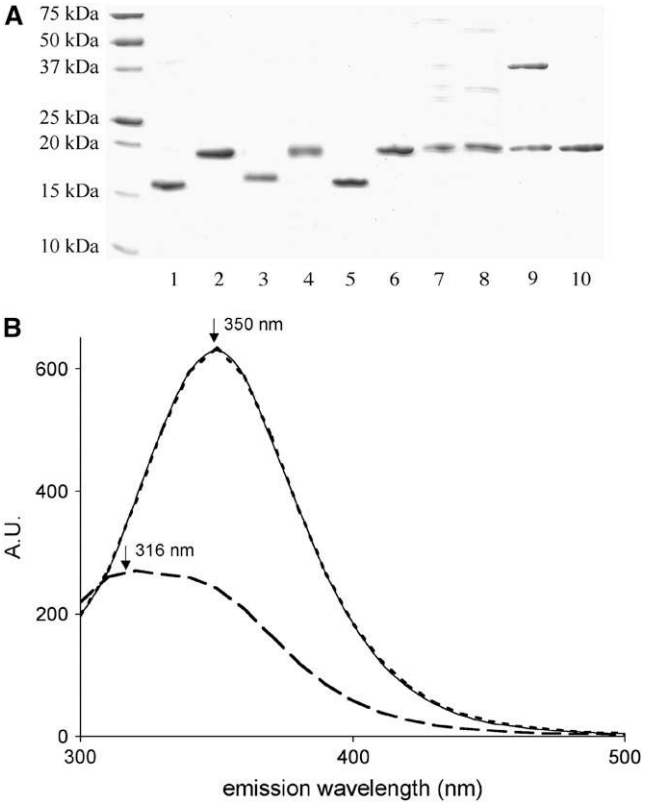

Figure 4. Effects of redox conditions on PtrcGpx3.2. A, The proteins were either oxidized with 30 mM H_2O_2 (lanes 1, 3, 5, 7, and 9) or reduced with 30 mM DTT (lanes 2, 4, 6, 8, and 10) and separated on 14% SDS-PAGE. Lanes 1 and 2, Gpx3.2; lanes 3 and 4, Gpx3.2 C107S; lanes 5 and 6, Gpx3.2 C136S; lanes 7 and 8, Gpx3.2 C155S; and lanes 9 and 10, Gpx3.2 C136S/155S. A total of 1 μg of protein was loaded per lane. B, Fluorescence emission spectrum of PtrcGpx3.2 in different redox conditions. Excitation was set at 290 nm. All spectra were recorded for 4 μM PtrcGpx3.2 concentration in 30 mM Tris, pH 8, 1 mM EDTA at room temperature. Untreated sample spectrum is figured in continuous line, spectrum for sample treated for 10 min with 250 μM DTT is figured in discontinuous line, and sample treated with DTT then incubated for 1 min with 250 μM H_2O_2 is figured in dotted line. Maximum emission peaks are indicated.

states, the mutation of Cys-155 prevents modification of Trp fluorescence and thus of the formation of the disulfide bond. No change of fluorescence was observed for PtrcGpx3.2 C107S, while a shift, attributed to the formation of a Cys-136-Cys-155 disulfide bond, was visible on SDS-PAGE. Altogether, these results indicate that Trp fluorescence is modified only when the peroxidatic Cys (Cys-107) and the resolving Cys (Cys-155) are involved in the formation of a disulfide bond.

Gel-filtration experiments performed with reduced or untreated PtrcGpx3.2 showed that it consistently elutes with an apparent molecular mass of 38 kD, corresponding to a homodimer (data not shown). As the protein migrates as a monomer (around 19 kD) under both reducing and nonreducing conditions during denaturing SDS-PAGE, the dimer observed during gel filtration cannot involve an intermolecular disulfide and must be stabilized by noncovalent forces (e.g. electrostatic or hydrophobic interactions).

Redox titrations of PtrcGpx3.2 using redox equilibration buffers composed either of defined mixtures of oxidized and reduced DTT or of defined mixtures of GSH plus oxidized GSH (GSSG) are most readily interpreted in terms of a single disulfide/dithiol redox couple per monomer, with a midpoint redox potential (E_m) value of 295 ± 10 mV at pH 7.0 (Fig. 5). Redox titrations (data not shown) over a more positive range than that shown in Figure 5 (i.e. E_h values ranging from −250 mV to −80 mV), in which defined mixtures of GSH plus GSSG were used as redox equilibration buffers, demonstrated that no additional more positive dithiol/disulfide couple is present in the protein. As Cys-136 is not involved in catalysis and the protein is not present as a disulfide-linked covalent dimer, one can conclude that the value observed corresponds to an intramolecular disulfide bridge linking Cys-107 to Cys-155.

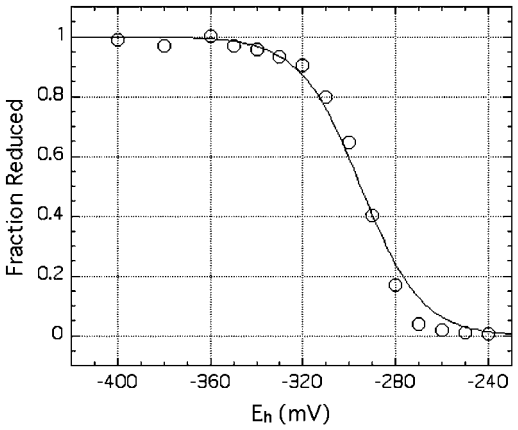

Figure 5. Redox titration of PtrcGpx3.2. The titration was carried out as described in "Materials and Methods" using a total DTT concentration of 2 mM in the redox buffer and with a redox equilibration time of 2 h.

Expression of Prx in Plant Organs and in Stress Conditions

We first performed an in silico analysis based on ESTs found in the DOE JGI database and found 191 ESTs coding for poplar Gpxs (Table I). The different isoforms are not equally represented among these ESTs; PtrcGpx3.2 seems to be the most frequently expressed gene, with 85 corresponding ESTs (i.e. approximately 45%). We also found 48 ESTs for PtrcGpx1, 10 for PtrcGpx2, 23 for PtrcGpx3.1, 17 for PtrcGpx4, and eight for PtrcGpx5. These results were combined with a semiquantitative reverse transcription (RT)-PCR approach. As these genes belong to the Prx family, we have studied the transcript expression pattern of all Gpxs together with the nine Prxs existing in poplar in seven different tissues (roots, young leaves, expanded leaves, fruits, stems, petioles, and stamen). For most genes, we have been able to find specific hybridizing areas. However, we were sometimes unable to distinguish some closely related sequences (i.e. Prx Q1 and Q2 or 2-Cys Prx A and B). In these two cases, we used nonspecific primers able to amplify both transcripts (Prx Q1 and Q2 or 2-Cys Prx A and B), but we were also able to define one primer to specifically amplify one gene (Prx Q1 and 2-Cys Prx A). From the difference between these two amplifications, the expression of the second gene can be deduced. For example, as the 2-Cys Prx A is only expressed in expanded leaves, we can estimate from the 2-Cys Prx A and B expression profile that 2-Cys Prx B is expressed in fruits, stems, petioles, and stamens and possibly in expanded leaves. All the genes exhibit different expression patterns, but there is at least one gene expressed in each organ tested (Fig. 6A). These data, coupled with the in silico analysis, are indicative of a broad distribution and expression of Prxs in plants, at least at the transcript level. Nevertheless, the multiplicity of Prx genes can be explained by some specificity in the expression pattern. For example, out a total of 17 genes, only three (coding for PtrcGpx2, PtrcGpx 3.1, and PtrcPrx IIE) are expressed at detectable levels in roots under the growth conditions used. One gene (PtrcPrx IIE) encodes a plastidic protein, another (PtrcGpx3.1) appears to encode a cytosolic Gpx, and the third (PtrcGpx2) appears to encode a secreted Gpx. In contrast, all the genes are expressed in expanded leaves. Given the specificity of the two chloroplastic Gpxs (PtrcGpx1 or PtrcGpx3.2) for a Trx of the y type as an electron donor, it was also of interest to examine the expression patterns of these two poplar Trxs. Both Trx y1 and y2 were found to be expressed in all tissues tested, and thus their role cannot simply be restricted to serving as specific reductants for plastidial Gpxs.

To get a deeper view of the expression of *Gpx* genes, we used both microarray data available using Genevestigator and the results presented by Rodriguez Milla et al. (2003) to follow the expression pattern of the different Arabidopsis Gpx genes in the whole plant (Fig. 6B; Zimmermann et al., 2004). Based on the

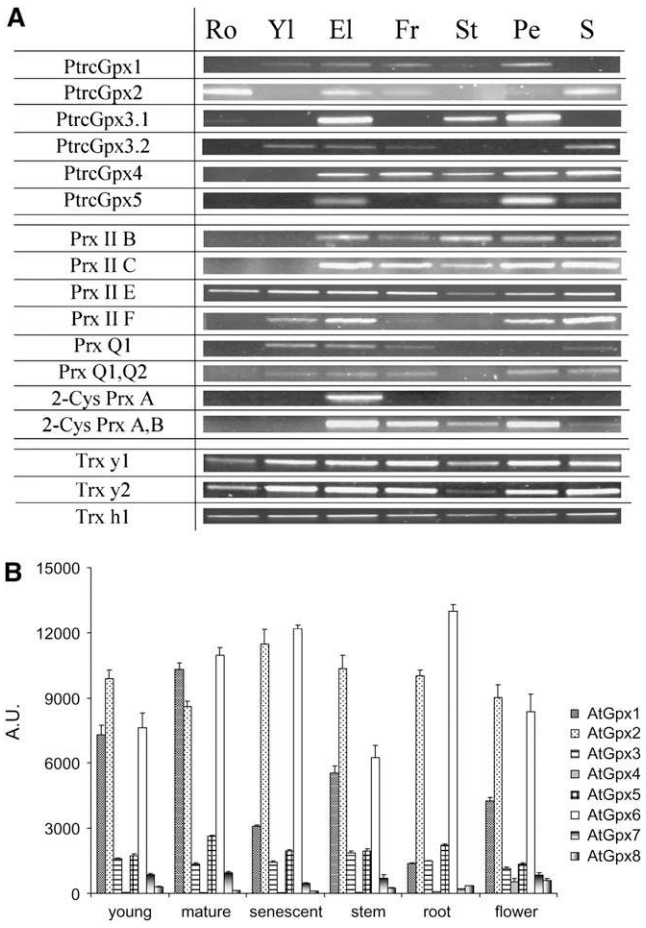

Figure 6. Prx transcript expression profiles. A, Expression of Gpx, Prx, and Trx y transcripts. RT-PCR reactions were performed with RNA extracted from various poplar organs (Ro, Root; Yl, young leaf; El, expanded leaf; Fr, fruit; St, stem; Pe, petiole; and S, stamen), loaded on 0.8% agarose gel, and stained with ethidium bromide. B, AtGpx gene expression pattern in the different plant organs, as compiled from microarray data available using the GeneAtlas function of Genevestigator (Zimmermann et al., 2004). Accession numbers: AtGpx1, At2g25080; AtGpx2, At2g31570; AtGpx3, At2g43350; AtGpx4, At2g48150; AtGpx5, At3g63080; AtGpx6, At4g11600; AtGpx7, At4g31870; and AtGpx8, At1g63460.

results of Rodriguez Milla et al. (2003), AtGpxs1 to 7 are expressed in all tissues analyzed, except AtGpx2, which does not seem to be expressed in dry seeds. AtGpx4 and 7 are the less expressed genes, as they were only detected by RT-PCR and few or no ESTs are found for these genes (Rodriguez Milla et al., 2003). Using Genevestigator, we observed that AtGpx1, AtGpx2, and AtGpx6, respectively homologous to PtrcGpx1, PtrcGpx2, and PtrcGpx3.2, were highly expressed in all organs or tissues analyzed (i.e. in young, expanded, and senescent leaves, as well as in stems, roots, and flowers), while AtGpx3, AtGpx5, AtGpx7, and AtGpx8, and especially AtGpx4, generally show a low expression level in these organs. Nevertheless, as expected for a chloroplastic protein, AtGpx1 is preferentially expressed in green tissues (young and expanded leaves, stems, and flowers). The main difference between the two sources concerns the expression of AtGpx6, which was found to be low in all organs except dry seeds by northern blot, while microarray data indicates a strong expression in all organs.

Using an antibody raised against purified recombinant PtrcGpx3.2, we first checked its specificity against the recombinant proteins. It reacts with all five recombinant proteins (which incidentally all migrate at slightly different positions on SDS-PAGE) but only faintly with PtrcGpx1 and 5 and more strongly with PtrcGpx2, 3.2, and 4 (Fig. 7A). This antibody is thus specific for Gpx as a whole, including the sixth protein, PtrcGpx3.1, which is very similar to PtrcGpx3.2 but does not discriminate between the isoforms. We could, however, differentiate at least two isoforms with two slightly different molecular masses in poplar protein extracts. The higher molecular mass band seems specific to roots, and because the signals obtained with the extracts from all the other organs tested have a similar size, they could thus correspond to a single isoform that we cannot identify for the reasons explained above (Fig. 7B).

In Arabidopsis (Fig. 7C), two bands of different sizes arising from two or more different isoforms have been detected in almost all organs, except roots. The protein(s) of smaller molecular mass is most easily detected in leaves and flowers, while in contrast the protein(s) of higher molecular mass is present in stems and roots and to a lesser extent in leaves and flowers. Using proteins extracted from purified leaf chloroplasts, only the lower band was detected (data not shown). Given the fact that AtGpx7 is weakly expressed at the transcriptional level, only the other two predicted chloroplastic proteins (i.e. AtGpx1 and AtGpx6) are likely to be detectable. Thus, we conclude that the lower band consists predominantly of AtGpx1 and/or AtGpx6. The upper band is likely to arise from the presence of AtGpx2, as it is not a chloroplastic protein and because AtGpx3, AtGpx4, AtGpx5, and AtGpx8 also seem to be weakly expressed at the transcriptional level. We next

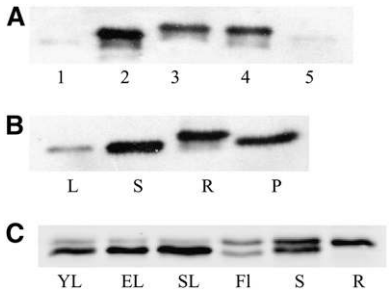

Figure 7. Gpx expression in poplar and Arabidopsis organs. A, Specificity of PtrcGpx3.2 antibodies. A total of 30 ng of each recombinant poplar Gpx (PtrcGpx1 to 5) was used. B, Distribution of Gpx expression in different poplar organs. L, Leaf; S, stem; R, root; and P, petiole (30 μg of total proteins loaded). C, Distribution of Gpx expression in different Arabidopsis organs. YL, Young leaf; EL, expanded leaf; SL, senescent leaf; Fl, flower; S, stem; and R, root (30 μg of total proteins loaded).

investigated the abundance of these proteins in stress situations (Fig. 8). Gpx abundance as a function of time was followed after infection of poplar by the agent of poplar rust, the fungus *Melampsora larici-populina*, and using two different isolates, a virulent one that induces a compatible reaction and an avirulent one that induces an incompatible reaction (Fig. 8A). As is the case for untreated leaf extracts, a single band is visible. During the incompatible reaction, the expression of Gpx increased greatly 2 h after infection and even more after 48 h. The pattern of expression during the compatible reaction is strikingly different, with a lower protein level observed at both 2 h after infection and then again at 24 h after infection but with levels very similar to those seen prior to infection found at all other times. Because this expression pattern is surprising, we have analyzed the expression of Trx h1, which is constitutively expressed and was never found to vary with stress, as a control (N. Rouhier, unpublished data). As expected, the Trx h1 abundance is not dependent on the pathogen infection, regardless of which fungal isolate was used.

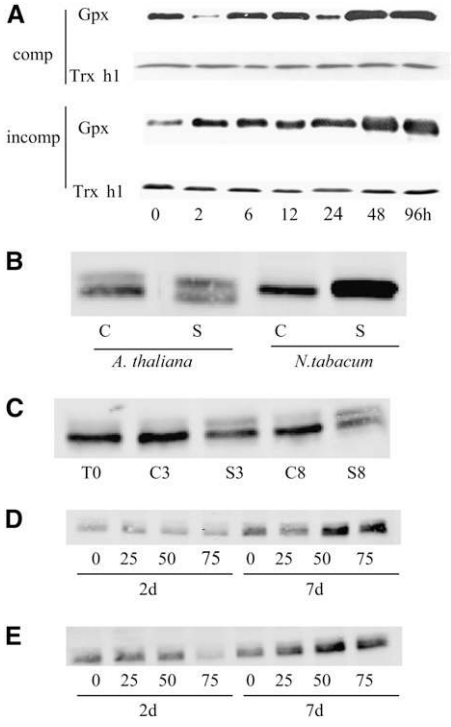

Figure 8. Gpx protein expression in poplar and Arabidopsis subjected to biotic or abiotic stresses. A, Abundance of poplar Gpxs during infection by the rust fungus *M. larici-populina* between 0 and 96 h after a compatible or an incompatible reaction. The variation of Trx h1 amount was used as a control. B, Abundance of Gpxs in young leaves of Arabidopsis or tobacco plants exposed to a water deficit of 6 d (S) compared to control plants (C). C, Abundance of Gpxs in expanded leaves of Arabidopsis plants exposed to photooxidative stress (low temperature [8°C] combined to high light [1,400 μE m^{-2} s^{-1}; S]) for 3 or 8 d compared to control plants (C). D, Abundance of Gpxs in expanded leaves of Arabidopsis plants subjected to various concentrations of cadmium (0, 25, 50, or 75 μM added to hydroponic plants) for 2 or 7 d. E, Abundance of Gpxs in expanded leaves of Arabidopsis plants subjected to various concentrations of copper (0, 25, 75, or 150 μM added to hydroponic plants) for 2 or 7 d. Each western blot (30 μg of protein were loaded per lanes) was done at least in duplicates with two independent treatments.

In addition, we followed Gpx levels in young leaves from Arabidopsis or tobacco (*Nicotiana tabacum*) plants submitted to various abiotic stresses. After 6 d of water deficit, the intensity of the lower band decreased, while that of the upper band increased (Fig. 8B). This was even more pronounced in young tobacco leaves subjected to the same conditions with an increased intensity of the Gpx signal, which could correspond to the presence of one or more Gpx isoforms (Fig. 8B). Similar profiles were observed using expanded leaves (data not shown). In plants subjected to photooxidative stress (Fig. 8C), the amount of the two proteins varied in the opposite way; the intensity of the upper band increased slightly under stress conditions in expanded leaves, whereas the intensity of the lower band decreased after 3 or 8 d of treatment.

In plants exposed to metal stresses induced by application of various concentrations of cadmium or copper for 2 and 7 d, only the amount of the lower M_r protein(s) detected is modified. It decreased at 150 μM copper after 2 d (Fig. 8E) but increased strongly after 7 d at cadmium concentrations of 50 and 75 μM (Fig. 8D) and at copper concentrations of 25, 75, and 150 μM (Fig. 8E).

Subcellular Localization of PtrcGpx1 and PtrcGpx3.2

PtrcGpx2 and PtrcGpx5 are predicted to be secreted but were not studied here, as we were unable to amplify the 5′ end coding for their N-terminal extensions from either cDNA libraries or genomic DNA. Although Arabidopsis and *O. sativa* homologs possess this extension, it is not yet clear whether these extensions really belong to the cDNA or are annotation or assembly errors. PtrcGpx4 and PtrcGpx3.1 contain neither an N-terminal extension nor known C-terminal signals, suggesting that the proteins are cytosolic. To determine the subcellular localization of PtrcGpx1 and PtrcGpx3.2, the 5′ portions of the open reading frame encoding only the N-terminal parts were fused to the sequence coding for a GFP. The recombinant pCK GFP S65C plasmids were then used to transiently transform tobacco cells by bombardment. In the guard cells shown here, it appears that Gpx1 is specifically targeted to chloroplasts and that Gpx3.2 is directed both to chloroplasts and mitochondria (Fig. 9). Similar results were obtained in mesophyll cells (data not shown).

DISCUSSION

As more and more genomes are sequenced and annotated, it is now clear that multigenic families are very common in organisms. Here, we describe the

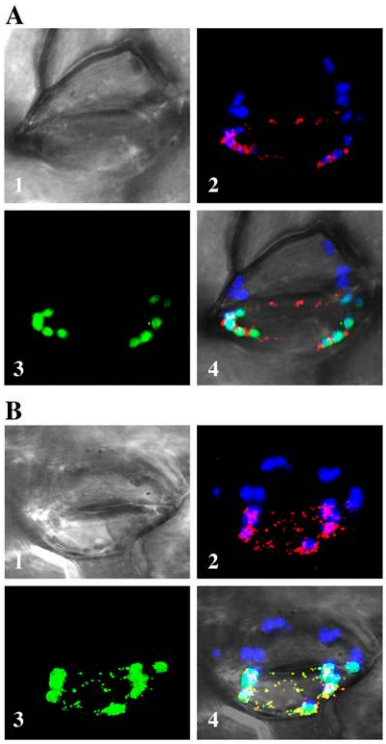

Figure 9. Subcellular localization of PtrcGpx1 (A) and PtrcGpx3.2 (B). N-terminal extensions of the two Gpxs were fused to the GFP and used to bombard tobacco cells. The pictures presented here are guard cells. 1, Visible light; 2, autofluorescence of chlorophyll (blue) and mitochondrial marker (red); 3, fluorescence of the construction; and 4, merged images.

existence of six Gpx isoforms in the model tree poplar. By comparison, eight and five Gpx isoforms are present in the genome of Arabidopsis and *O. sativa*, respectively. The number of *Gpx* genes thus varies among species, probably because of gene duplication events. A continuing challenge is to understand why so many genes or proteins with similar functions are needed in plants. To answer this question, both the abundance and localization of the proteins and the substrate specificities of these enzymes were studied. As a result of our study, it is now clear that the poplar enzymes originally named Gpxs are reduced by Trxs rather than by GSH and belong to the Prx family. This large family thus includes 15 different Prxs in poplar.

Substrate and Electron Donor Specificities

The poplar Gpxs do not exhibit any difference in the reduction of H_2O_2 compared to complex hydroperoxides (COOH and tBOOH), as the catalytic efficiencies (k_{cat}/K_m) vary only over a 20-fold range (i.e. from 2.6 to 53 $\times$ 10^3 M^{-1} s^{-1}). The reduction of complex peroxides is consistent with a role for Gpxs (and for Prxs in general) that complements other systems, like catalases or ascorbate peroxidases, which specifically reduce H_2O_2. The catalytic efficiencies of poplar Gpxs lie in the range previously described for other Prxs. Rouhier et al. (2004) determined kinetics parameters for poplar chloroplastic Prx Q, with k_{cat} around 1 s^{-1} and k_{cat}/K_m of 10^3 to 10^4 M^{-1} s^{-1}, depending on the substrate considered. Horling et al. (2002) reported an activity of Prx IIC that is in the same range. Previous studies (Herbette et al., 2002; Jung et al., 2002; Tanaka et al., 2005) also indicate that plant or yeast Gpxs may display kinetic parameters similar to those of the other classes of the broad Prx family. The catalytic efficiencies reported to date for Gpxs and Prxs are far lower than those of catalases or ascorbate peroxidases, but they are likely to reduce a broader range of substrates than these two enzymes. Gpxs may also provide the graduated response necessary for the metabolic fine tuning in case of oxidative stress, as has been demonstrated in the interaction with transcription factors (Delaunay et al., 2002). All these data are consistent with a possible role for Gpxs and Prxs in ROS detoxification in plant cells and, as has been demonstrated in other organisms, in redox signaling (Delaunay et al., 2002; Rhee et al., 2005; Vivancos et al., 2005).

In so far as the electron donor specificity of poplar Gpxs is concerned, these enzymes seem to behave like previously characterized plant Gpx in that they can be reduced by Trxs, as earlier demonstrated for some plant Gpx (Herbette et al., 2002; Jung et al., 2002) but not at all by GSH. We have also demonstrated that Grxs, which can provide a pathway for disulfide reduction alternative to the Trx pathway, are unable to reduce poplar Gpxs. However, because only five Grxs belonging to the same subgroup were tested, the possibility exists that one or more other members of the large Grx family might serve as an effective electron donor to Gpx. The oxidation-reduction titrations carried out in this study (see Fig. 5) provide a thermodynamic basis for this donor specificity. The intramolecular Cys-107/Cys-155 disulfide present in the oxidized PtrcGpx3.2 was shown to have an E_m value at pH 7.0 of -295 ± 10 mV. While reduction of this PtrcGpx3.2 disulfide by Trxs, which have E_m values ranging from -275 mV to -330 mV (Brehelin et al., 2003; Collin et al., 2003), would be expected to be thermodynamically

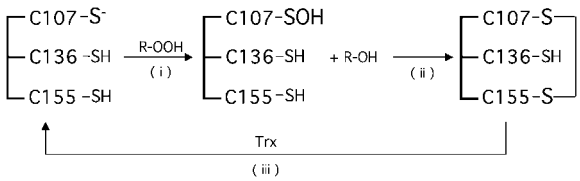

Figure 10. Proposed catalytic and Trx-dependent recycling mechanisms for poplar Gpx: (i) nucleophilic attack of Cys-107 on peroxide (ROOH) leading to the formation of a sulfenic acid and the concomitant release of an alcohol; (ii) formation of an intramolecular disulfide bridge between Cys-107 and Cys-155; and (iii) reduction of the intramolecular disulfide bridge by Trx leading to a reduced enzyme and an oxidized Trx.

favorable, the more positive E_m values of GSH (E_m = −245 mV at pH 7.0) and plant Grxs (E_m values around −180 mV; N. Rouhier, unpublished data) would make reduction of the PtrcGpx3.2 disulfide thermodynamically unfavorable.

The question of which Trx is the actual physiological electron donor for different Gpxs remains unsettled. Taking the Trx h family as an example, we were unable to establish a preference between Trx h1, h3, and h5 in in vitro assays. It was previously demonstrated that neither a poplar Trx h2 nor an Arabidopsis Trx o were able to serve as reductants to PtrcGpx3.2 (Gelhaye et al., 2004), and thus the identity of the physiological reductant for this mitochondrial Gpx remains unclear.

Considering the putative secreted isoforms, namely PtrcGpx2 and PtrcGpx5, we found that Trx h5 is able to reduce PtrcGpx5 in a catalytic manner (data not shown). Juarez-Diaz et al. (2005) recently showed that a homolog of poplar Trx h5 was secreted by *Nicotiana alata* cells. Assuming that PtrcGpx5 is actually secreted, these two proteins could be part of an extracellular redox signaling system. Pignocchi and Foyer (2003) suggested that changes in the apoplastic redox state could be sensed by a system involving dithiol-disulfide exchanges. Secreted Gpxs may be candidates as apoplastic redox sensors.

There are at least 11 chloroplastic Trxs in Arabidopsis (NtrC, CDSP32, Trx x, Trx y1 and y2, Trx f1 and f2, Trx m1, m2, m3, and m4) and even more in poplar (E. Gelhaye, unpublished data). Although we did not test the efficiency of the bimodular Trxs (NtrC and CDSP32), it appears that only the two Trx y are able to efficiently support the activity of PtrcGpx1 and PtrcGpx3.2. These chloroplastic Trxs all have very similar E_m, and so the specificities observed must arise from properties of the Trxs other than their E_m values (e.g. the distributions of surface charges and of surface hydrophobic patches). In a previous study, it was found in Arabidopsis that only Trx x is able to reduce 2-Cys Prx, and Trx y is the most efficient electron donor to Prx Q (Collin et al., 2004). It is then likely that the major function of x-type and y-type chloroplastic Trxs is the reduction of chloroplastic Prxs (this family includes 2-Cys Prxs, Prx Q, Prx IIE, and Gpxs). The f-type Trxs are specifically needed in the regulation of chloroplastic metabolism (in particular, through the activation of FBPase and of the CF_1 ATP synthase), but they can also reduce 2-Cys Prxs and Prx Q. The m-type Trxs may play a dual role, regulating metabolism through control of NADP-dependent malate dehydrogenase and also serving as possible reductants for 2-Cys Prx and Prx Q (Collin et al., 2003). Overall, this would constitute a system with partial redundancy that could be linked to each subcellular compartment redox state.

Using the digital northern function of Genevestigator online database (https://www.genevestigator.ethz.ch; Zimmermann et al., 2004), we noticed that the mRNA profiles of the Arabidopsis ortholog of PtrcGpx1 (AtGpx1, accession no. At2g25080) are more closely related to that of AtTrx y1 (accession no. At1g76760) than to that of AtTrx y2 (accession no. At1g43560). This may indicate which of the two y-type Trxs is likely to be the favored electron donor to this enzyme in vivo. As there are also two isoforms of Trx y in poplar, the situation might be similar. RT-PCR experiments showed that the two genes (Trx y1 and y2) are expressed in all the organs tested, and thus at the moment one cannot identify specific and distinct roles for the two isoforms.

Catalytic Mechanism and Trx-Mediated Recycling Process

When starting this work, one question was to determine whether one, two, or three Cys were involved in the reactions catalyzed by plant Gpxs. Although yeast Gpx2 had been shown to possess a Trx-dependent activity, involving only the two Cys equivalent to Cys-107 and Cys-155 in poplar (Tanaka et al., 2005). Jung et al. (2002) had previously suggested a catalytic mechanism involving three conserved Cys residues for a Chinese cabbage (*Brassica napus*) Gpx. This proposal was based on mass spectrometry data that showed that a disulfide bridge could be formed between the Cys corresponding to poplar Cys-136 and Cys-155 (Jung et al., 2002) and on their observation that the mutated protein equivalent to PtrcGpx C136S retained only 30% of the activity displayed by the wild-type enzyme. Here, we show that, although three Cys are absolutely conserved in all Gpxs from higher plants, only two are involved both in catalysis and in the Trx-dependent regeneration. Indeed, three observations support this conclusion: (1) the stoichiometry of the reaction catalyzed by the wild-type enzyme is consistently 1:1 (in terms of peroxide reduced to enzyme oxidized) and never 2:1; (2) the mutated PtrcGpx3.2 C136S is as active as PtrcGpx3.2; and (3) we have detected only one disulfide bridge when titrating PtrcGpx3.2. Another characteristic of these enzymes is a shift during migration under SDS-PAGE similar to that previously reported by Tanaka et al. (2005) for yeast Gpx2, as the redox state of the protein is altered. Both the redox-dependent shift in SDS-PAGE migration properties and the redox-dependent changes in the Trp fluorescence parameters of the proteins clearly indicate that Cys-155 is required for the formation of an intramolecular disulfide with Cys-107. One additional piece of evidence that Gpx belongs to the Prx family is its formation of noncovalent dimers. Indeed, the only plant Prx for which a structure is known is a homodimer with a conserved interface found in other nonplant Prx structures (Echalier et al., 2005). A structural study designed to determine the structural determinants responsible for substrate binding, for dimerization, and to elucidate a possible role for the highly conserved Cys-136 is currently under way.

Unlike the case for many other eukaryotic Prx characterized so far, we did not observe the formation of overoxidized forms of Gpx. Indeed, the stoichiometry of the reaction catalyzed by Gpxs is consistently 1, the

activity measured in the presence of the Trx system is linear with time, and H_2O_2-treated proteins do not undergo the mass increment expected for sulfinic or sulfonic formation (data not shown). We thus propose a three-step reaction mechanism for plant Gpxs similar to the one used by Prx Q, with two Cys forming an intramolecular disulfide bridge in the oxidized state (Fig. 10). These steps are: (1) a nucleophilic attack of the catalytic Cys (Cys-107) on the peroxide with the release of an alcohol and the concomitant formation of a sulfenic acid; (2) an attack of the sulfenic acid by Cys-155 and formation of an intramolecular disulfide bridge between Cys-107 and Cys-155; and (3) a reduction of the disulfide bridge by Trx.

Expression and Localization of Gpx in Plants

We analyzed the expression of all the Prxs in poplar organs. All the members of this family are expressed at the transcriptional level in at least one of the organs tested, with a specific expression pattern for each of them. Gpxs are likely to be present in all organs and in nearly all cell compartments, suggesting a redundancy with the Prxs identified previously. Interestingly, many isoforms are expressed in flowers or in fruits, but their precise physiological function is yet unknown. Nevertheless, to explain the need for proteins with identical functions, we can imagine that some genes could be expressed in specific conditions under stress, for example, or could be temporally regulated.

When poplar leaves are subjected to a biotic stress (infection by the rust fungus *M. larici-populina*), the abundance of these proteins is modified. This is in line with previous observations that the levels of Prx Q, Prx IIC, and Prx IIF but not of 2-Cys Prx are modified in this situation (Rouhier et al., 2004; Gama et al., 2007). Abiotic stress conditions (water deficit, photooxidative, and metal stresses) also induce modifications of the Gpx levels. The amount of isoform(s) of lower molecular masses is especially modified, generally decreasing in water deficit and photooxidative stress but strongly increasing in the presence of toxic metals such as cadmium or copper. In the case of photooxidative stress, it was previously shown that among members of the Prx family, only the amount of Prx Q increased in this situation, whereas the level of Prx IIE and 2-Cys Prx remained unchanged (Havaux et al., 2005). In our case, the amount of chloroplastic Gpx(s) decreased, suggesting there is a fine control and a functional specialization among members of the same family. It was previously demonstrated at the transcript levels that AtGpx2, AtGpx5, and AtGpx6 were strongly and rapidly increased in Arabidopsis plants treated with 200 μM of $FeSO_4$ or $CuSO_4$ (Rodriguez Milla et al., 2003). Other studies provided evidence for an increased Gpx activity in plants treated with copper (Ali et al., 2006) or nickel (Gajewska and Sklodowska, 2006) but decreased activity in the presence of cadmium (Aravind et al., 2005). The conclusion, based on our results and those of others, that Gpxs are Trx-dependent enzymes suggests that the GSH-dependent peroxidase activity found in these studies corresponds to the peroxidase activity of GSH *S*-transferases. Taken as a whole, the results presented above provide evidence at the protein level that supports the conclusions based on previous observations in mRNA studies that Gpx are involved in stress responses and especially in response to metals. For example, it was previously demonstrated that overexpression of a Gpx from *C. reinhardtii* both in the cytosol and in the chloroplast and overexpression of a tomato (*Lycopersicon esculentum*) Gpx in yeast and plant increased tolerance to oxidative stress (Chen et al., 2004; Yoshimura et al., 2004).

Another possible explanation for the redundancy of Trx peroxidases as a whole could be linked to their subcellular distribution. Using GFP fusion, we demonstrated that two Gpxs (PtrcGpx1 and 3.2) are localized in chloroplast, one of these (PtrcGpx3.2) being also targeted to mitochondria. This dual targeting is not unusual, having already been observed for some other antioxidant proteins (GSH reductase [GR], monodehydroascorbate reductase, and ascorbate peroxidase; Chew et al., 2003). The plastidic localization of PtrcGpx1 was expected, as a pea (*Pisum sativum*) Gpx homolog was previously shown to be imported into chloroplasts (Mullineaux et al., 1998). Only one other plant Gpx was previously localized experimentally. This protein, from tomato, called GPXle-1 and homologous to PtrcGpx3.1, was found in the cytosol near the plasma membrane and to a lesser extent in the cell wall of some leaf cells (Herbette et al., 2004).

Adding the results of this investigation to the previously available data on distribution of Prxs, eight poplar Prxs are now known to be expressed in plastids (Prx IIE, 2-Cys Prx A and B, Prx Q1 and 2, and PtrcGpx1 and PtrcGpx3.2), two in mitochondria (Prx IIF and PtrcGpx3.2), three in the cytosol (Prx IIB, Prx IIC, and PtrcGpx3.1), one in the nucleus (Prx 1-Cys), and two predicted to be directed to the secretory pathways (PtrcGpx2 and PtrcGpx5), assuming that these proteins indeed contain an N-terminal extension. This situation is slightly different from Arabidopsis, in which there is only one Prx Q but an additional cytosolic Prx II and eight Gpxs instead of the six found in poplar.

MATERIALS AND METHODS

Materials

H_2O_2, tBOOH, COOH, NADPH, GSH, and GR from yeast (*Saccharomyces cerevisiae*) were purchased from Sigma.

Expression of Poplar Gpxs in Various Organs

RT-PCR

Semiquantitative RT-PCR experiments were used to estimate the distribution of Gpx, Prx, and y-type Trx transcripts in various poplar (*Populus trichocarpa*) organs. Total RNA isolation was performed with the RNeasy Plant Mini kit (Qiagen) from approximately 100 mg of various frozen tissues obtained from 4-month-old poplar plants (young and expanded leaves, roots,

stems, and petioles) or from older poplar trees (fruits and stamen). To remove contaminating DNA, the samples were treated with DNAseI (Qiagen). Except for the stem (for which we used 300 ng), a total of 1 μg of total RNA was used to generate cDNAs by RT using the Omniscript RT kit (Qiagen). These products were used as templates for subsequent PCR reactions using the primers described in Supplemental Table S2. The program used was as follows: 94°C for 3 min and 35 cycles of 94°C for 30 s, 54°C for 45 s, and 72°C for 1 min 45 s. The primers used were sometimes identical to those used for the cloning experiments (Gpx1, 2, and 4; 1-Cys Prx). When two open reading frames were very similar (e.g. Gpx3.1 or 3.2; Prx IIC, D, and E; Prx Q1 and Q2, Prx 2-Cys A and B, Trx y1 and 2), we used one or two new primers hybridizing in the 3′ or 5′ part of mRNAs, sometimes in combination with one of the cloning primers. When no selective amplification was possible for one isoform out of a pair of very close sequences, primers that can hybridize the two forms were used. In the case of Gpx5, the amplification was done with two specific internal primers. The Trx h1 gene from poplar, which is expressed in all tissues tested, was amplified simultaneously and used as a control. The PCR fragments were then loaded on a 0.8% agarose gel.

Western Blotting

Infection of poplar leaves with either avirulent or virulent fungal isolates of the rust fungus *Melampsora larici-populina* was carried out as described in Rouhier et al. (2004). Arabidopsis (*Arabidopsis thaliana*) plants subjected to water deficit and photooxidative or metal stresses were treated as described in Vieira dos Santos et al. (2005) and Gama et al. (2007). A total of 30 μg of proteins was loaded per lane on 15% denaturing SDS-PAGE then transferred onto polyvinylidene difluoride membranes (Millipore) when using poplar protein extracts or onto nitrocellulose membranes (Pall) for Arabidopsis extracts. Antibodies raised against PtrcGpx3.2 were diluted 1,500×. Detection of proteins recognized by antibodies on polyvinylidene difluoride membranes was done by autoradiography and using the Odyssey Infrared Imager from LICOR in the case of nitrocellulose membranes.

Cloning and Site-Directed Mutagenesis

After identification in the databases (see "Results"), the nucleotide sequences of PtrcGpx2, 3.2, and 4 were then amplified by PCR using the primers described in Supplemental Table S2 from a *Populus tremula* × *trichocarpa* cv Beaupre poplar root cDNA library (Kohler et al., 2003), and PtrcGpx1 and PtrcGpx5 were amplified directly from isolated *Escherichia coli* colonies containing the cDNA of interest (gift from Dr. Gunnar Wingsle, University of Umeå, Sweden). Each of the three Cys of the mature PtrcGpx3.2, at positions 107, 136, and 155, respectively, were replaced individually by Ser using site-directed mutagenesis following a procedure described in Jacquot et al. (1997). The double mutant PtrcGpx3.2 C136S, C155S, which only contains the first Cys, was also generated and cloned. After digestion with the *Nco*I and *Bam*HI restriction enzymes, PCR fragments were inserted into the pET-3 d expression plasmid.

Production and Purification of Recombinant Gpxs

The recombinant plasmids obtained were used to transform the BL21(DE3) pSBET strain of *E. coli* (Schenk et al., 1995). The bacteria were then grown to a final volume of approximately 3.2 L at 37°C, and protein production was induced during exponential phase by adding 100 μM isopropyl-β-D-thiogalactoside. For PtrcGpx3.2, the amount of soluble protein increased when bacteria were grown overnight at 30°C without induction by isopropyl-β-D-thiogalactoside. The bacteria were harvested by centrifugation at 5,000 rpm for 20 min and then resuspended in TE buffer (Tris-HCl 30 mM, pH 8.0, EDTA 1 mM). Cells were broken by sonication, and all Gpxs were found in the soluble fraction after high speed centrifugation, except for PtrcGpx2, which was present mostly in inclusion bodies.

The insoluble portion of PtrcGpx2 was first denatured by resuspending the pellet in TE buffer containing 8 M urea. The soluble proteins obtained after centrifugation at 16,000 rpm for 30 min were then renatured slowly by two successive dialyses of 6 h, first against TE buffer containing 0.5 M urea and then against TE buffer alone. A centrifugation step (30 min at 16,000 rpm) was performed after each dialysis to remove denatured proteins. For the soluble isoforms, ammonium sulfate fractionation was used as the first step in the purification procedure. For all of these soluble Gpxs, most of the protein precipitated between 40% and 80% saturation.

The next purification step, used for all Gpxs, was gel filtration carried out on ACA44 (Biosepra), equilibrated in TE buffer containing 200 mM NaCl. After removing NaCl by ultrafiltration, the Gpx fractions were loaded onto a DEAE-Sephacel ion-exchange column (Amersham). A gradient ranging from 0 to 400 mM NaCl was used for the elution of PtrcGpx2, 4, and 5, whereas PtrcGpx1 and 3.2 passed through the column. After dialysis and concentration, the proteins were analyzed for purity by SDS-PAGE and stored frozen at −20°C in TE buffer.

Biochemical Characterization of Poplar Gpx

NADPH-Coupled Spectrophotometric Method

These experiments were performed at 30°C and were based on monitoring the decrease in absorbency at 340 nm arising from NADPH oxidation. All Gpxs were tested using this method and showed similar catalytic parameters. The catalytic properties of PtrcGpx3.2 and its cysteinic mutants (PtrcGpx3.2 C107S, C136S, C155S, and C136/155S; 200 nM) were investigated in more detail and were tested using either a reduced Trx-generating system (3 μM Arabidopsis recombinant NTRb and various concentrations of Trx h1, h3, and h5 from poplar), or the Grx system (0.5 units GR, 1 mM GSH, and 100 μM Grx C4), or GSH alone (0.5 units GR, 2 mM GSH) as possible electron donors. These assays were carried out in a total volume of 500 μL in 30 mM Tris-HCl, pH 8, buffer, 1 mM EDTA, and 200 μM NADPH. The catalytic parameters for one substrate were measured by varying its concentration at saturating concentrations of the other substrate (typically between 1 and 100 μM for Trx, and between 40 μM and 12 mM for the peroxides [H_2O_2, tBOOH, or COOH]).

FOX Colorimetric Method

The reduction of peroxides by PtrcGpx1 and PtrcGpx3.2, the two chloroplastic isoforms of poplar, was also followed using the FOX colorimetric method (Wolff, 1994). All the monomodular chloroplastic Trxs from Arabidopsis were assayed as possible electron donors. A 50-μL reaction mixture contained 2 μM of recombinant PtrcGpx1 or 3.2, 500 μM DTT, and 10 μM of Trx f1, f2, m1, m2, m3, m4, x, y1, or y2 recombinant proteins from Arabidopsis, purified as described in Collin et al. (2003). The reaction was started by adding the peroxide (either H_2O_2, tBOOH, or COOH) to a final concentration of 400 μM. At different times, 5 μL of the reaction mixture was added to 495 μL of the colorimetric reagent and the absorbency read at 560 nm after 30 min incubation in the dark.

Stoichiometry of the Reaction

The stoichiometry of the reaction was also measured using the FOX method with a known concentration of reduced enzyme (typically 100 μM or 200 μM) in the absence of any other reductants and in the presence of 400 or 500 μM peroxides. The residual amount of peroxide remaining after reduction by a known amount of protein was titrated after completion of the reaction (30 min). The enzyme was reduced with a large excess of DTT (10 mM), which was removed, prior to the assay, by two successive dialyses, each time against 1 L of TE buffer.

Oligomerization and Redox State of Gpx

The redox state of PtrcGpx3.2 and of the mutated proteins was analyzed by incubating the proteins with either 30 mM DTT or 30 mM H_2O_2 for 30 min before separating them on 14% acrylamide SDS-PAGE gels. It was also analyzed by following intrinsic Trp emission fluorescence using a Cary Eclipse fluorimeter (Varian). Measurements were recorded at room temperature in a 1- × 1-cm cuvette. The excitation wavelength was set to 290 nm (5 nm bandpass). Emitted light was detected at 90° between 300 and 500 nm. Spectra of a 1-mL solution containing 4 μM of various PtrcGpxs were recorded before adding successively 250 μM DTT and then 250 μM H_2O_2.

The native oligomerization state of PtrcGpx3.2 was determined both in oxidized (i.e. as isolated) or reduced (30-min incubation with 20 mM DTT) conditions using an ACA 44 gel-filtration column (5 × 75 cm) and proteins of known molecular masses as standards (bovine serum albumin, ovalbumin, and chymotrypsinogen; Sigma).

Intracellular Localization via GFP Fusion

The nucleotide sequences corresponding to the predicted N-terminal extension of PtrcGpx1 and PtrcGpx3.2 were cloned into the *Nco*I and *Bam*HI sites of pCK-GFP S65C using the primers detailed in Supplemental Table S2 as

PtrcGpx1 FOR GFP, PtrcGpx1 REV GFP, PtrcGpx3.2 FOR GFP, and PtrcGpx3.2 REV GFP. These primers were designed to amplify the sequences corresponding to the predicted signal peptides of Gpx1 (from MASLPF to TEKSVH) and Gpx3.2 [from M(A) LTSRS to SQSSPQ; see Fig. 1]. The PCR fragments were fused to GFP at the *Bam*HI site, resulting in chimeric proteins where the N-terminal extensions of the two Gpxs are present at the N terminus of enhanced GFP, under the control of a double 35S promoter (Menand et al., 1998). *Nicotiana benthamiana* cells were then transfected by bombardment of leaves with tungsten particles coated with plasmid DNA, and images were obtained with a Zeiss LSM510 confocal microscope.

E_m Determination

Oxidation-reduction titrations, using the fluorescence of the adduct formed between the protein and mBBr to monitor the thiol content of the protein, were carried out at ambient temperature as described previously (Krimm et al., 1998; Hirasawa et al., 1999). The reaction mixtures contained 100 μg of protein in 100 mM MOPS buffer, pH 7.0, containing defined mixtures of oxidized and reduced DTT to set the ambient potential (E_h). Identical titrations were obtained at total DTT concentrations of 1, 2, and 4 mM. The titration behavior was also independent of redox equilibration time over the range from 1.5 to 3 h. Titrations at more positive (E_h) values were carried out in a similar fashion, except that GSH replaced DTT in the redox equilibration buffer total GSH plus GSSG concentration of 2 mM. The ambient potential was set by varying the ratio of GSSG to GSH as described previously (Setterdahl et al., 2000). Redox equilibration times of either 2 or 3 h were used.

Sequence data from this article can be found in the GenBank/EMBL data libraries under accession numbers CF936448 (Gpx1), DT518382 (Gpx2), DT516214 (Gpx3.2), DT487747 (Gpx4), and BU863119 (Gpx5).

Supplemental Data

The following materials are available in the online version of this article.

Supplemental Table S1. Structure of the poplar Gpx genes.

Supplemental Table S2. Primers used in this study.

Received September 4, 2006; accepted October 11, 2006; published October 27, 2006.

LITERATURE CITED

Agrawal GK, Rakwal R, Jwa NS, Agrawal VP (2002) Effects of signaling molecules, protein phosphatase inhibitors and blast pathogen (*Magnaporthe grisea*) on the mRNA level of a rice (*Oryza sativa* L.) phospholipid hydroperoxide glutathione peroxidase (OsPHGPX) gene in seedling leaves. Gene **283:** 227–236

Ali MB, Hahn EJ, Paek KY (2006) Copper-induced changes in the growth, oxidative metabolism, and saponin production in suspension culture roots of *Panax ginseng* in bioreactors. Plant Cell Rep **25:** 1122–1132

Aravind P, Prasad MN (2005) Modulation of cadmium-induced oxidative stress in *Ceratophyllum demersum* by zinc involves ascorbate-glutathione cycle and glutathione metabolism. Plant Physiol Biochem **43:** 107–116

Avery AM, Willetts SA, Avery SV (2004) Genetic dissection of the phospholipid hydroperoxidase activity of yeast gpx3 reveals its functional importance. J Biol Chem **279:** 46652–46658

Boschi-Muller S, Azza S, Sanglier-Cianferani S, Talfournier F, Van Dorsselear A, Branlant G (2000) A sulfenic acid enzyme intermediate is involved in the catalytic mechanism of peptide methionine sulfoxide reductase from *Escherichia coli.* J Biol Chem **275:** 35908–35913

Boschi-Muller S, Olry A, Antoine M, Branlant G (2005) The enzymology and biochemistry of methionine sulfoxide reductases. Biochim Biophys Acta **1703:** 231–238

Brehelin C, Meyer EH, de Souris JP, Bonnard G, Meyer Y (2003) Resemblance and dissemblance of Arabidopsis type II peroxiredoxins: similar sequences for divergent gene expression, protein localization, and activity. Plant Physiol **132:** 2045–2057

Chen S, Vaghchhipawala Z, Li W, Asard H, Dickman MB (2004) Tomato phospholipid hydroperoxide glutathione peroxidase inhibits cell death induced by Bax and oxidative stresses in yeast and plants. Plant Physiol **135:** 1630–1641

Chew O, Whelan J, Millar AH (2003) Molecular definition of the ascorbate-glutathione cycle in Arabidopsis mitochondria reveals dual targeting of antioxidant defenses in plants. J Biol Chem **278:** 46869–46877

Churin Y, Schilling S, Borner T (1999) A gene family encoding glutathione peroxidase homologues in *Hordeum vulgare* (barley). FEBS Lett **459:** 33–38

Collin V, Issakidis-Bourguet E, Marchand C, Hirasawa M, Lancelin JM, Knaff DB, Miginiac-Maslow M (2003) The Arabidopsis plastidial thioredoxins: new functions and new insights into specificity. J Biol Chem **278:** 23747–23752

Collin V, Lamkemeyer P, Miginiac-Maslow M, Hirasawa M, Knaff DB, Dietz KJ, Issakidis-Bourguet E (2004) Characterization of plastidial thioredoxins from Arabidopsis belonging to the new y-type. Plant Physiol **136:** 4088–4095

Criqui MC, Jamet E, Parmentier Y, Marbach J, Durr A, Fleck J (1992) Isolation and characterization of a plant cDNA showing homology to animal glutathione peroxidases. Plant Mol Biol **18:** 623–627

Delaunay A, Pflieger D, Barrault MB, Vinh J, Toledano MB (2002) A thiol peroxidase is an H_2O_2 receptor and redox-transducer in gene activation. Cell **111:** 471–481

Depege N, Drevet J, Boyer N (1998) Molecular cloning and characterization of tomato cDNAs encoding glutathione peroxidase-like proteins. Eur J Biochem **253:** 445–451

Echalier A, Trivelli X, Corbier C, Rouhier N, Walker O, Tsan P, Jacquot JP, Aubry A, Krimm I, Lancelin JM (2005) Crystal structure and solution NMR dynamics of a D (type II) peroxiredoxin glutaredoxin and thioredoxin dependent: a new insight into the peroxiredoxin oligomerism. Biochemistry **44:** 1755–1767

Eshdat Y, Holland D, Faltin Z, Ben-Hayyim G (1997) Plant glutathione peroxidases. Physiol Plant **100:** 234–240

Finkemeier I, Goodman M, Lamkemeyer P, Kandlbinder A, Sweetlove LJ, Dietz KJ (2005) The mitochondrial type II peroxiredoxin F is essential for redox homeostasis and root growth of *Arabidopsis thaliana* under stress. J Biol Chem **280:** 12168–12180

Fu LH, Wang XF, Eyal Y, She YM, Donald LJ, Standing KG, Ben-Hayyim G (2002) A selenoprotein in the plant kingdom: mass spectrometry confirms that an opal codon (UGA) encodes selenocysteine in *Chlamydomonas reinhardtii* gluthathione peroxidase. J Biol Chem **277:** 25983–25991

Gajewska E, Sklodowska M (2006) Effect of nickel on ROS content and antioxidative enzyme activities in wheat leaves. Biometals (in press)

Gama F, Keech O, Eymery F, Finkemeier I, Gelhaye E, Gardeström P, Dietz KJ, Rey P, Jacquot JP, Rouhier N (2007) The mitochondrial type II peroxiredoxin from poplar. Physiol Plant (in press)

Gelhaye E, Rouhier N, Gerard J, Jolivet Y, Gualberto J, Navrot N, Ohlsson PI, Wingsle G, Hirasawa M, Knaff DB, et al (2004) A specific form of thioredoxin h occurs in plant mitochondria and regulates the alternative oxidase. Proc Natl Acad Sci USA **101:** 14545–14550

Havaux M, Eymery F, Porfirova S, Rey P, Dormann P (2005) Vitamin E protects against photoinhibition and photooxidative stress in *Arabidopsis thaliana.* Plant Cell **17:** 3451–3469

Hazebrouck S, Camoin L, Faltin Z, Strosberg AD, Eshdat Y (2000) Substituting selenocysteine for catalytic cysteine 41 enhances enzymatic activity of plant phospholipid hydroperoxide glutathione peroxidase expressed in *Escherichia coli.* J Biol Chem **275:** 28715–28721

Herbette S, Brunel N, Prensier G, Julien JL, Drevet JR, Roeckel-Drevet P (2004) Immunolocalization of a plant glutathione peroxidase-like protein. Planta **219:** 784–789

Herbette S, Lenne C, Leblanc N, Julien JL, Drevet JR, Roeckel-Drevet P (2002) Two GPX-like proteins from *Lycopersicon esculentum* and *Helianthus annuus* are antioxidant enzymes with phospholipid hydroperoxide glutathione peroxidase and thioredoxin peroxidase activities. Eur J Biochem **269:** 2414–2420

Hirasawa M, Schürmann P, Jacquot JP, Manier W, Jacquot P, Keryer E, Hartman FC, Knaff DB (1999) Oxidation-reduction properties of chloroplast thioredoxins, ferredoxin:thioredoxin reductase, and thioredoxin *f* -regulated enzymes. Biochemistry **38:** 5200–5205

Holland D, Faltin Z, Perl A, Ben-Hayyim G, Eshdat Y (1994) A novel plant glutathione peroxidase-like protein provides tolerance to oxygen radicals generated by paraquat in *Escherichia coli.* FEBS Lett **337:** 52–55

Horling F, König J, Dietz KJ (2002) Type II peroxiredoxin C, a member of the peroxiredoxin family of *Arabidopsis thaliana*: its expression and activity in comparison with other peroxiredoxins. Plant Physiol Biochem **40:** 491–499

Jacquot JP, Stein M, Suzuki A, Liottet S, Sandoz G, Miginiac-Maslow M (1997) Residue Glu-91 of Chlamydomonas reinhardtii ferredoxin is essential for electron transfer to ferredoxin-thioredoxin reductase. FEBS Lett **400:** 293–296

Juarez-Diaz JA, McClure B, Vazquez-Santana S, Guevara-Garcia A, Leon-Mejia P, Marquez-Guzman J, Cruz-Garcia F (2005) A novel thioredoxin h is secreted in Nicotiana alata and reduces S-RNase in vitro. J Biol Chem **281:** 3418–3424

Jung BG, Lee KO, Lee SS, Chi YH, Jang HH, Kang SS, Lee K, Lim D, Yoon SC, Yun DJ, et al (2002) A Chinese cabbage cDNA with high sequence identity to phospholipid hydroperoxide glutathione peroxidases encodes a novel isoform of thioredoxin-dependent peroxidase. J Biol Chem **277:** 12572–12578

Kang SG, Jeong HK, Suh HS (2004) Characterization of a new member of the glutathione peroxidase gene family in *Oryza sativa.* Mol Cells **17:** 23–28

Kohler A, Delaruelle C, Martin D, Encelot N, Martin F (2003) The poplar root transcriptome: analysis of 7000 expressed sequence tags. FEBS Lett **542:** 37–41

Krimm I, Lemaire S, Ruelland E, Miginiac-Maslow M, Jacquot J-P, Hirasawa M, Knaff DB, Lancelin J-M (1998) The single mutation W35A in the 35-40 redox site of *Chlamydomonas reinhardtii* thioredoxin *h* affects its biochemical activity and the pH dependence of C36-C39 ^{1}H-^{13}C NMR. Eur J Biochem **255:** 185–195

Kuzniak E, Sklodowska M (2005) Fungal pathogen-induced changes in the antioxidant systems of leaf peroxisomes from infected tomato plants. Planta **222:** 192–200

Li WJ, Feng H, Fan JH, Zhang RQ, Zhao NM, Liu JY (2000) Molecular cloning and expression of a phospholipid hydroperoxide glutathione peroxidase homolog in *Oryza sativa.* Biochim Biophys Acta **1493:** 225–230

Maiorino M, Gregolin C, Ursini F (1990) Phospholipid hydroperoxide glutathione peroxidase. Methods Enzymol **186:** 448–457

Menand B, Marechal-Drouard L, Sakamoto W, Dietrich A, Wintz H (1998) A single gene of chloroplast origin codes for mitochondrial and chloroplastic methionyl-tRNA synthetase in *Arabidopsis thaliana.* Proc Natl Acad Sci USA **95:** 11014–11019

Mullineaux PM, Karpinski S, Jimenez A, Cleary SP, Robinson C, Creissen GP (1998) Identification of cDNAs encoding plastid-targeted glutathione peroxidase. Plant J **13:** 375–379

Noctor G, Foyer CH (1998) Ascorbate and glutathione: keeping active oxygen under control. Annu Rev Plant Physiol Plant Mol Biol **49:** 249–279

Novoselov SV, Rao M, Onoshko NV, Zhi H, Kryukov GV, Xiang Y, Weeks DP, Hatfield DL, Gladyshev VN (2002) Selenoproteins and selenocysteine insertion system in the model plant cell system, *Chlamydomonas reinhardtii.* EMBO J **21:** 3681–3693

Pedrajas JR, Miranda-Vizuete A, Javanmardy N, Gustafsson JA, Spyrou G (2000) Mitochondria of *Saccharomyces cerevisiae* contain one-conserved cysteine type peroxiredoxin with thioredoxin peroxidase activity. J Biol Chem **275:** 16296–16301

Pignocchi C, Foyer CH (2003) Apoplastic ascorbate metabolism and its role in the regulation of cell signalling. Curr Opin Plant Biol **6:** 379–389

Prabhakar R, Vreven T, Morokuma K, Musaev DG (2005) Elucidation of the mechanism of selenoprotein glutathione peroxidase (GPx)-catalyzed hydrogen peroxide reduction by two glutathione molecules: a density functional study. Biochemistry **44:** 11864–11871

Rhee SG, Kang SW, Jeong W, Chang TS, Yang KS, Woo HA (2005) Intracellular messenger function of hydrogen peroxide and its regulation by peroxiredoxins. Curr Opin Cell Biol **17:** 183–189

Rodriguez Milla MA, Maurer A, Rodriguez Huete A, Gustafson JP (2003) Glutathione peroxidase genes in *Arabidopsis* are ubiquitous and regulated by abiotic stresses through diverse signaling pathways. Plant J **36:** 602–615

Roeckel-Drevet P, Gagne G, Tourvieille de Labrouhe D, Dufaure JP, Nicolas P, Drevet JR (1998) Molecular characterization, organ distribution and stress-mediated induction of two glutathione peroxidase-encoding mRNAs in sunflower (*Helianthus annuus*). Physiol Plant **103:** 385–394

Rouhier N, Couturier J, Jacquot JP (2006) Genome-wide analysis of plant glutaredoxin systems. J Exp Bot **57:** 1685–1696

Rouhier N, Gelhaye E, Gualberto JM, Jordy MN, De Fay E, Hirasawa M, Duplessis S, Lemaire SD, Frey P, Martin F, et al (2004) Poplar peroxiredoxin Q: a thioredoxin-linked chloroplast antioxidant functional in pathogen defense. Plant Physiol **134:** 1027–1038

Rouhier N, Gelhaye E, Sautiere PE, Brun A, Laurent P, Tagu D, Gerard J, de Fay E, Meyer Y, Jacquot JP (2001) Isolation and characterization of a new peroxiredoxin from poplar sieve tubes that uses either glutaredoxin or thioredoxin as a proton donor. Plant Physiol **127:** 1299–1309

Rouhier N, Jacquot JP (2002) Plant peroxiredoxins: alternative hydroperoxide scavenging enzymes. Photosynth Res **74:** 259–268

Rouhier N, Jacquot JP (2005) The plant multigenic family of thiol peroxidases. Free Radic Biol Med **38:** 1413–1421

Schenk PM, Baumann S, Mattes R, Steinbiss HH (1995) Improved high-level expression system for eukaryotic genes in *Escherichia coli* using T7 RNA polymerase and rare Arg tRNAs. Biotechniques **19:** 196–198

Setterdahl AT, Goldman BS, Hirasawa M, Jacquot P, Smith AJ, Kranz RG, Knaff DB (2000) Oxidation-reduction properties of disulfide-containing proteins of the *Rhodobacter capsulatus* cytochrome *c* biogenesis system. Biochemistry **39:** 10172–10176

Sugimoto M, Sakamoto W (1997) Putative phospholipid hydroperoxide glutathione peroxidase gene from *Arabidopsis thaliana* induced by oxidative stress. Genes Genet Syst **72:** 311–316

Sztajer H, Gamain B, Aumann KD, Slomianny C, Becker K, Brigelius-Flohe R, Flohe L (2001) The putative glutathione peroxidase gene of *Plasmodium falciparum* codes for a thioredoxin peroxidase. J Biol Chem **276:** 7397–7403

Tanaka T, Izawa S, Inoue Y (2005) GPX2, encoding a phospholipid hydroperoxide glutathione peroxidase homologue, codes for an atypical 2-Cys peroxiredoxin in *Saccharomyces cerevisiae.* J Biol Chem **280:** 42078–42087

Vieira Dos Santos C, Cuine S, Rouhier N, Rey P (2005) The Arabidopsis plastidic methionine sulfoxide reductase B proteins: sequence and activity characteristics, comparison of the expression with plastidic methionine sulfoxide reductase A, and induction by photooxidative stress. Plant Physiol **138:** 909–922

Vivancos AP, Castillo EA, Biteau B, Nicot C, Ayte J, Toledano MB, Hidalgo E (2005) A cysteine-sulfinic acid in peroxiredoxin regulates H2O2-sensing by the antioxidant Pap1 pathway. Proc Natl Acad Sci USA **102:** 8875–8880

Wolff SP (1994) Ferrous ion oxidation of ferric ion indicator xylenol orange for measurement of hydroperoxides. Methods Enzymol **233:** 182–189

Yoshimura K, Miyao K, Gaber A, Takeda T, Kanaboshi H, Miyasaka H, Shigeoka S (2004) Enhancement of stress tolerance in transgenic tobacco plants overexpressing Chlamydomonas glutathione peroxidase in chloroplasts or cytosol. Plant J **37:** 21–33

Zimmermann P, Hirsch-Hoffmann M, Hennig L, Gruissem W (2004) GENEVESTIGATOR: Arabidopsis microarray database and analysis toolbox. Plant Physiol **136:** 2621–2632